NUCL SCI TECH (2018) 29:18
https://doi.org/10.1007/s41365-018-0364-6

Wetting behaviors of methanol, ethanol, and propanol on hydroxylated SiO_2 substrate

Xue-Chuan Nie[1,2] · **Bo Zhou**[3] · **Chun-Lei Wang**[1] · **Hai-Ping Fang**[1]

Received: 23 September 2017 / Revised: 20 November 2017 / Accepted: 4 December 2017 / Published online: 25 January 2018

Abstract Water molecules could form a liquid droplet on the water monolayer on a specific solid surface, which has been referred to as "ordered water monolayer that does not completely wet water" at room temperature. In contrast to the water molecules, the family of alcohol molecules has the same OH polar head and various lengths of their hydrophobic nonpolar tail; the length of the hydrophobic tail can affect the hydrophobic effect. In this study, using molecular dynamics simulations, we investigated the wetting behaviors of methanol, ethanol, and propanol molecules adsorbed on a SiO_2 surface. The results showed that the methanol, ethanol, and propanol molecules could form an ordered monolayer on the SiO_2 surface and a droplet on top of this monolayer, with different contact angles. The differences in the contact angles were attributed to the differences in the interactions between the alcohol monolayer and droplet.

Keywords Wetting behavior · Alcohol · SiO_2 · Molecular dynamics simulation

1 Introduction

The assembling and wetting behavior of small molecules, such as water and alcohol molecules, are important for applications in various fields including interfacial science [1, 2], energy conversion [3], environmental protection [4, 5], biological science [6–8], and nanodevices [9]. Owing to its importance, the adsorption of alcohol molecules on various mineral surfaces such as SiO_2 [10–13], mica [14], Al_2O_3 [15, 16], calcite [17, 18], and sapphire [19] has been extensively investigated.

Our previous study showed that the small water molecules could form an ordered monolayer on a solid surface with particular charge patterns. In addition, a liquid droplet could form on top of the monolayer [20–24]; it has been referred to as "ordered water monolayer that does not completely wet water" at room temperature. Similar phenomena have been observed on several real solid surfaces such as metals (Pt [25, 26] and Pd [26]), sapphire [27], talc [28], hydroxylated Al_2O_3 and SiO_2 [29]. The family of alcohol molecules has the same OH polar head, which can form hydrogen bonds, and various lengths of the hydrophobic nonpolar tail, which indicates the more complex adsorption behavior on solid surfaces than that of water. The length of the hydrophobic tail can affect the solvation behavior of the amphiphilic molecules at the nanoscale, as the hydrophobic effect is sensitive to the

---

This study was supported by the National Natural Science Foundation of China (Nos. U1532260, 11674345, and 11504032), Key Research Program of Chinese Academy of Sciences (Nos. KJZD-EW-M03 and QYZDJ-SSW-SLH019), Youth Innovation Promotion Association CAS (Grant Number 2014233), Shanghai Supercomputer Center of China, Computer Network Information Center of Chinese Academy of Sciences, and Special Program for Applied Research on Super Computation of the NSFC-Guangdong Joint Fund (the second phase).

✉ Chun-Lei Wang
wangchunlei@sinap.ac.cn

[1] Division of Interfacial Water and Key Laboratory of Interfacial Physics and Technology, Shanghai Institute of Applied Physics, Chinese Academy of Sciences, Shanghai 201800, China

[2] University of Chinese Academy of Sciences, Beijing 100049, China

[3] School of Electronic Engineering, Chengdu Technological University, Chengdu 611730, China

hydrophobic tail length [30, 31]. The effect of the length of the hydrophobic tail on the wetting behavior of the family of alcohol molecules is not yet understood, though it has been shown that an ethanol droplet can form on an ordered monolayer on a SiO_2 surface [32, 33].

In this study, we investigated molecular wetting behaviors of alcohol molecules with various hydrophobic tail lengths (0.143, 0.297, and 0.451 nm for methanol, ethanol, and propanol, respectively) on a hydroxylated SiO_2 surface using molecular dynamics simulations. The results showed that methanol, ethanol, and propanol could form ordered monolayers on the SiO_2 surface, and that corresponding droplets could form on the monolayers. The contact angle of the ethanol droplet is the largest, attributed to the weakest adhesion interaction between the ethanol droplet and monolayer.

2 Computational methods

The (111)-face of β-cristobalite SiO_2 was used as the substrate, as in our previous study [33]. The CLAYFF force field was used to parameterize SiO_2 [33, 34]. The Lorentz–Berthelot mixing rules were used for the unlike-pair interactions. First, alcohol droplets of pure methanol, ethanol, and propanol were deposited on SiO_2 substrates. Each of the pure methanol, ethanol, and propanol droplets contained 1500 molecules of the corresponding alcohol. The parameters of the alcohol molecules were taken from the OPLS-AA force field [35–37]. The MD simulation software GROMACS version 5.0.2 was employed for the simulations [38]. The simulation box size was $12.350\ \text{nm} \times 14.176\ \text{nm} \times 20.000\ \text{nm}$. The total simulation time of each system was 20 ns; the data of the last 10 ns of the trajectory were used for the analysis. All other simulation parameter settings were the same with those in our previous study [33]. The criteria for the hydrogen bonds were distance (O–O) smaller than 3.5 Å and angle (H–O···O) smaller than 30°.

3 Results and discussion

Our simulations show that all three types of alcohol molecules exhibit similar behaviors on the SiO_2 substrate. Figure 1 shows side-view snapshots of the simulation results for methanol, ethanol, and propanol. All three types of alcohol can assemble to an ordered monolayer with a droplet on top of it. The detailed configurations of the monolayers in Fig. 1 show that the alcohol molecules in the monolayers stand upright on the SiO_2 substrate, with the OH groups pointing downwards and CH_3 groups pointing upwards. The top-view snapshots in Fig. 2 show that each of the three types of alcohol molecules in the monolayers is arranged in an ordered rhombic structure.

The numbers of hydrogen bonds formed between alcohol molecules and between alcohol molecules and SiO_2 are shown in Fig. 3. The results showed that each methanol, ethanol, and propanol molecule in the monolayers can form 1.84, 1.92, and 1.93 hydrogen bonds with the SiO_2 surface. Each alcohol molecule could form at most two hydrogen bonds with SiO_2. Therefore, hydrogen bonds could not be formed between alcohol molecules in the monolayer or between the monolayer and droplet. In other words, the formation of hydrogen bonds between the monolayer and SiO_2 surface prevents the formation of hydrogen bonds between the monolayer and droplet. This explains why the alcohol droplet can form on the monolayer, which is consistent with the results in our previous study [33].

In order to describe their morphology, we calculated the density distributions of the droplets, as shown in Fig. 4. First, the droplet was divided into small units with dimensions of $0.1\ \text{nm} \times 0.1\ \text{nm} \times 0.1\ \text{nm}$. Then, the number of alcohol molecules in each unit was calculated according to the geometrical center of each alcohol molecule. The density distribution was averaged over the range of 10–20 ns of the simulation trajectory. The density distributions were employed to determine the liquid–vapor interface of the droplet as follows: (1) the density of the droplet was analyzed, from its interior to the surface; (2) if the density at a given position was below 1/2 of the bulk density, that position was considered to be at the liquid–vapor interface of the droplet. The contact angle of the droplet was calculated according to the interface of the droplet. Figure 5 shows that the contact angles of the methanol, ethanol, and propanol droplets are 36°, 58°, and 54°, respectively. The contact angle of the ethanol droplet is the largest among the three types of alcohol droplets.

The modified Young–Dupre equation can be expressed as [39]:

$$\gamma_{\mathrm{L}}(1+\cos\theta) = -\Phi, \qquad (1)$$

where γ_{L} is the surface tension of the liquid, θ is the contact angle, and Φ is the interaction potential energy per unit area between the liquid droplet and substrate. The surface tensions of methanol, ethanol, and propanol are very similar (at 25 °C, the surface tensions of methanol, ethanol, and propanol are 22.51, 21.82, and 21.22 mN/m, respectively) [40]. Therefore, the contact angle is mainly determined by the interaction potential energy. The interaction potential energy between the alcohol droplet and monolayer is shown in Fig. 5, which shows that the interaction energy between the droplet and monolayer of ethanol is the largest, among the three types of alcohol. Based on Eq. (1) and the interaction energy, we derive that the contact angle

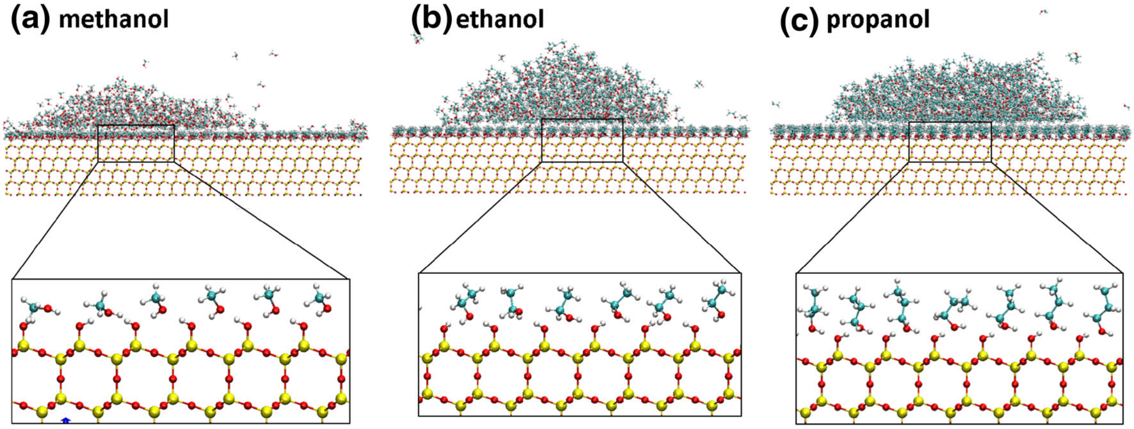

Fig. 1 (Color online) Side-view snapshots of the simulation results at 20 ns. Monolayer and droplet of **a** methanol, **b** ethanol, and **c** propanol on SiO_2. The bottom figures show detailed configurations of the monolayers

Fig. 2 (Color online) Top-view snapshots of the simulation results at 20 ns. Monolayer and droplet of **a** methanol, **b** ethanol, and **c** propanol

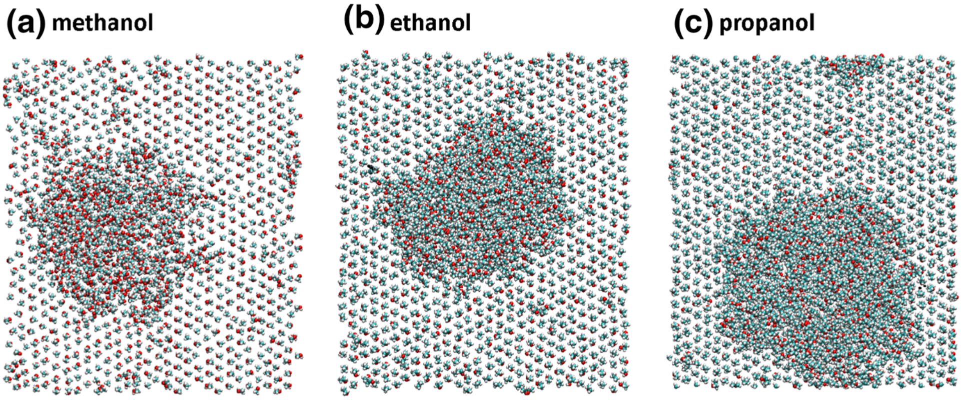

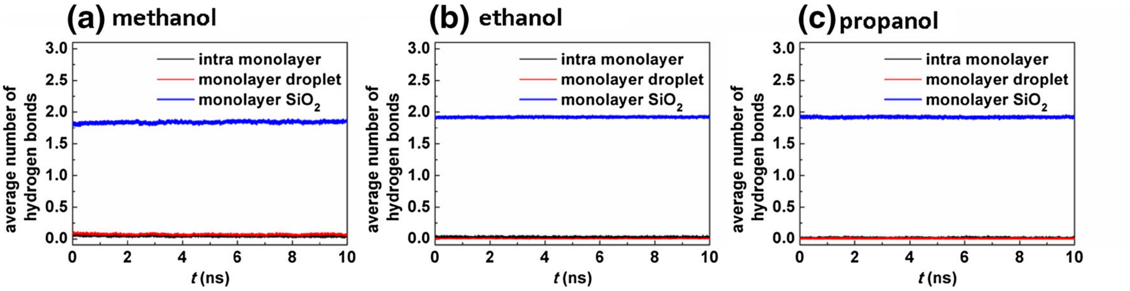

Fig. 3 (Color online) Average number of hydrogen bonds formed between alcohol molecules of **a** methanol, **b** ethanol, and **c** propanol and SiO_2. The black, red, and blue curves represent the hydrogen bonds formed between alcohol molecules in the monolayer, alcohol molecules in the monolayer and droplet, and alcohol molecules in the monolayer and SiO_2, respectively

θ of the ethanol droplet is the largest among the three types, consistent with the simulation results.

Further, we studied the orientation of the alcohol molecules in the monolayer and droplet by calculating the probability distributions of their tilt angle φ. It is defined as the angle between the line that connects the O atom of OH and C atom of CH_3, and z-axis [32]. Figure 6 shows that the probability distributions of φ of the three types of alcohol molecules have a similar profile; they all have a peak at $\varphi = 0°$. This indicates that the alcohol molecules in the monolayer favor an upright orientation with respect to the SiO_2 substrate. Owing to the strong attractive force between the OH groups of the alcohol molecules and SiO_2, the OH groups of the alcohol molecules point toward the SiO_2 surface, while the CH_3 groups point away from the SiO_2 surface. The probability distributions of φ of all three types decrease to zero with the increase of φ; the rate of decrease is different. For methanol, ethanol, and propanol, the probability distributions of φ decreases to zero for $\varphi > 120°$, 70°, and 45°. The probability distribution of φ

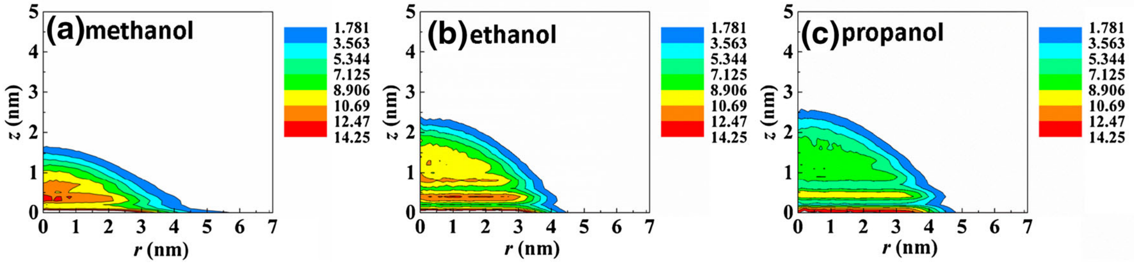

Fig. 4 (Color online) Number density distribution of the alcohol molecules in the droplets of **a** methanol, **b** ethanol, and **c** propanol; *r* denotes the distance from the center of mass of the droplet in the *xy* plane, and *z* denotes the height from the monolayer. The molecular number density is expressed in nm^{-3}

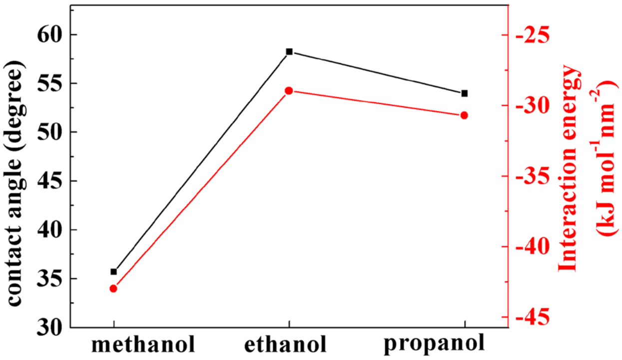

Fig. 5 (Color online) Contact angles of the alcohol droplets (black squares) and interaction energies between the droplets and corresponding monolayers (red circles)

of the propanol molecules decreases faster than that of the methanol and ethanol molecules, which indicates that the propanol molecules in the monolayer stand straighter than the methanol and ethanol molecules. The propanol molecules can arrange in a stable configuration on the SiO_2 surface, as the tail chain of the propanol molecules is longer than that of the methanol and ethanol molecules. The methanol molecules have a short chain length; hence, they can easily lie flat on the surface. Figure 6 shows that the probability distributions of φ of the alcohol molecules in the droplets are homogeneous, which indicates that the alcohol molecules in the droplets maintain a disordered orientation. The ordered orientation of the alcohol molecules in the monolayers leads to the ordered structures of the monolayers.

In order to provide further insights into the adsorption behavior of the alcohol molecules near the SiO_2 surfaces, we calculated the probability distributions of the CH_3 and OH groups of the methanol, ethanol, and propanol molecules along the *z*-axis (perpendicular to the SiO_2 surface). The results are shown in Fig. 7. The density distributions of the three types of alcohol molecules are similar. The distance between the first peaks of OH and CH_3 of the propanol molecules is 0.30 nm, larger than those of the methanol (0.09 nm) and ethanol (0.20 nm) molecules, as the size of the propanol molecule is larger than that of the methanol and ethanol molecules. Our previous study showed that the second peak of the C atom of CH_3 was near the first peak of the ethanol molecules, which indicates that a face-to-face orientation of CH_3 is formed between the monolayer and droplet [33]. In addition, Fig. 7 shows that for the propanol molecules, a face-to-face configuration of CH_3 is also formed between the monolayer and droplet. However, this face-to-face configuration of CH_3 for the methanol molecules is indistinct, mainly due to the small length of the methanol molecules.

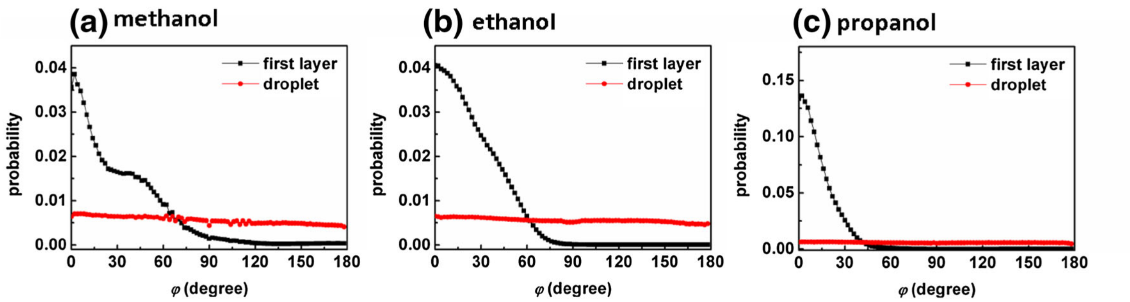

Fig. 6 (Color online) Distribution of the tilt angle φ of the **a** methanol, **b** ethanol, and **c** propanol molecules in the monolayer and droplet. The black squares and red circles represent the tilt angle φ distributions of the alcohol molecules in the monolayer and droplet, respectively

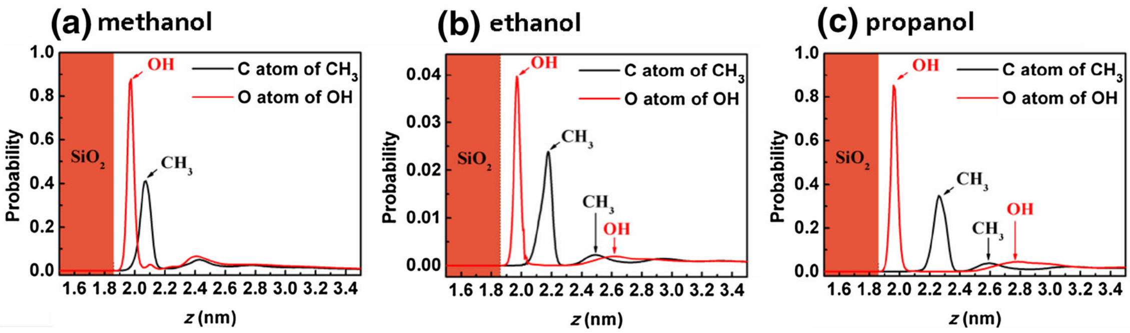

Fig. 7 (Color online) Probability distributions of the CH_3 and OH groups of the **a** methanol, **b** ethanol, and **c** propanol molecules along the *z*-axis (perpendicular to the SiO_2 surface). The black and red curves represent the probability distributions of the C atom in CH_3 and O atom in OH, of the alcohol molecules, respectively

4 Conclusion

Molecular dynamics simulations showed that the methanol, ethanol, and propanol molecules could form an ordered monolayer on the (111)-oriented hydroxylated β-cristobalite SiO_2 substrate and, in addition, a droplet could form on top of this ordered monolayer. The alcohol molecules in the monolayer favored the formation of hydrogen bonds with the SiO_2 substrate; this prevented the formation of hydrogen bonds with the droplet and led to the droplet formation. The contact angles of the methanol, ethanol, and propanol droplets were 36°, 58°, and 54°, respectively. The contact angle of the ethanol droplet was the largest among the three types of alcohol droplets, owing to the weakest adhesion interaction between the ethanol droplet and monolayer, consistent with the Young–Dupre equation.

References

1. C.K. Wu, L.J. Chen, Wetting behavior of mixtures of water and nonionic polyoxyethylene alcohol. Langmuir **21**, 6883–6890 (2005). https://doi.org/10.1021/la050691i
2. S.J. Shao, P. Guo, L. Zhao et al., Ordered water monolayer on ionic model substrates studied by molecular dynamics simulations. Nucl. Sci. Tech. **25**, 020502 (2014). https://doi.org/10.13538/j.1001-8042/nst.25.020502
3. G.L. Chang, D.G. Wang, Y.Y. Zhang et al., Ald-coated ultrathin al2o3 film on bivo4 nanoparticles for efficient pec water splitting. Nucl. Sci. Tech. **27**, 108 (2016). https://doi.org/10.1007/s41365-016-0122-6
4. P.I. Girginova, A.L. Daniel-da-Silva, C.B. Lopes et al., Silica coated magnetite particles for magnetic removal of hg 2+ from water. J. Colloid Interface Sci. **345**, 234–240 (2010). https://doi.org/10.1016/j.jcis.2010.01.087
5. H. Yang, R. Xu, X. Xue et al., Hybrid surfactant-templated mesoporous silica formed in ethanol and its application for heavy metal removal. J. Hazard. Mater. **152**, 690–698 (2008). https://doi.org/10.1016/j.jhazmat.2007.07.060
6. Y. Sun, L. Duan, Z. Guo et al., An improved way to prepare superparamagnetic magnetite-silica core-shell nanoparticles for possible biological application. J. Magn. Magn. Mater. **285**, 65–70 (2005). https://doi.org/10.1016/j.jmmm.2004.07.016
7. X. Ren, B. Zhou, C. Wang, Promoting effect of ethanol on dewetting transition in the confined region of melittin tetramer. Nucl. Sci. Tech. **23**, 252–256 (2012). https://doi.org/10.13538/j.1001-8042/nst.23.252-256
8. P. Wang, R.B. Zhong, M. Yuan et al., Mercury (ii) detection by water-soluble photoluminescent ultra-small carbon dots synthesized from cherry tomatoes. Nucl. Sci. Tech. **27**, 35 (2016). https://doi.org/10.1007/s41365-016-0038-1
9. W. Xu, Y.S. Tu, C.L. Wang et al., Water transport through t-shaped carbon nanotubes. Nucl. Sci. Tech. **22**, 307–310 (2011). https://doi.org/10.13538/j.1001-8042/nst.22.307-310
10. J.J. Karnes, E.A. Gobrogge, R.A. Walker et al., Unusual structure and dynamics at silica/methanol and silica/ethanol interfaces: a molecular dynamics and nonlinear optical study. J. Phys. Chem. B **120**, 1569–1578 (2015). https://doi.org/10.1021/acs.jpcb.5b07777
11. E.A. Gobrogge, R.A. Walker, Binary solvent organization at silica/liquid interfaces: preferential ordering in acetonitrile–methanol mixtures. J. Phys. Chem. Lett **5**, 2688–2693 (2014). https://doi.org/10.1021/jz500906d
12. M.R. Brindza, R.A. Walker, Differentiating solvation mechanisms at polar solid/liquid interfaces. J. Am. Chem. Soc. **131**, 6207–6214 (2009). https://doi.org/10.1021/ja810117f
13. A.R. Siler, R.A. Walker, Effects of solvent structure on interfacial polarity at strongly associating silica/alcohol interfaces. J. Phys. Chem. C **115**, 9637–9643 (2011). https://doi.org/10.1021/jp201153z
14. T. Cheng, H. Sun, Adsorption of ethanol vapor on mica surface under different relative humidities: a molecular simulation study. J. Phys. Chem. C **116**, 16436–16446 (2012). https://doi.org/10.1021/jp3020595
15. A. Phan, D.R. Cole, A. Striolo, Liquid ethanol simulated on crystalline alpha alumina. J. Phys. Chem. B **117**, 3829–3840 (2013). https://doi.org/10.1021/jp312238d
16. H.L. Rossetto, J. Bowen, K. Kendall, Adhesion of alumina surfaces through confined water layers containing various molecules. Langmuir **28**, 4648–4653 (2012). https://doi.org/10.1021/la2045064
17. I.S. Pasarín, M. Yang, N. Bovet et al., Molecular ordering of ethanol at the calcite surface. Langmuir **28**, 2545–2550 (2012). https://doi.org/10.1021/la2021758
18. D. Wu, A. Navrotsky, Probing the energetics of organic–nanoparticle interactions of ethanol on calcite. Proc. Natl. Acad. Sci. USA. **112**, 5314–5318 (2015). https://doi.org/10.1073/pnas.1505874112

19. J. Sung, G.A. Waychunas, Y.R. Shen, Surface-induced anisotropic orientations of interfacial ethanol molecules at air/sapphire($1\bar{1}02$) and ethanol/sapphire($1\bar{1}02$) interfaces. J. Phys. Chem. Lett **2**, 1831–1835 (2011). https://doi.org/10.1021/jz2006397
20. C. Wang, H. Lu, Z. Wang et al., Stable liquid water droplet on a water monolayer formed at room temperature on ionic model substrates. Phys. Rev. Lett. **103**, 137801 (2009). https://doi.org/10.1103/PhysRevLett.103.137801
21. C.L. Wang, H.P. Fang, "Ordered water monolayer that does not completely wet water" at room temperature and molecular-scale hydrophilicity (in chinese). Sci. China-Phys. Mech. Astron **46**, 74–83 (2016). https://doi.org/10.1360/SSPMA2015-00603
22. C. Wang, Y. Yang, H. Fang, Recent advances on "ordered water monolayer that does not completely wet water" at room temperature. Sci. China-Phys. Mech. Astron **57**, 802–809 (2014). https://doi.org/10.1007/s11433-014-5415-3
23. C. Qi, B. Zhou, C. Wang et al., A nonmonotonic dependence of the contact angles on the surface polarity for a model solid surface. Phys. Chem. Chem. Phys. **19**, 6665–6670 (2017). https://doi.org/10.1039/c6cp08275k
24. P. Guo, Y. Tu, J. Yang et al., Water-cooh composite structure with enhanced hydrophobicity formed by water molecules embedded into carboxyl-terminated self-assembled monolayers. Phys. Rev. Lett. **115**, 186101 (2015). https://doi.org/10.1103/PhysRevLett.115.186101
25. D.T. Limmer, A.P. Willard, P. Madden et al., Hydration of metal surfaces can be dynamically heterogeneous and hydrophobic. Proc. Natl. Acad. Sci. USA. **110**, 4200–4205 (2013). https://doi.org/10.1073/pnas.1301596110
26. Z. Xu, Y. Gao, C. Wang et al., Nanoscale hydrophilicity on metal surfaces at room temperature: coupling lattice constants and crystal faces. J. Phys. Chem. C **119**, 20409–20415 (2015). https://doi.org/10.1021/acs.jpcc.5b04237
27. J. Lützenkirchen, R. Zimmermann, T. Preočanin et al., An attempt to explain bimodal behaviour of the sapphire c-plane electrolyte interface. Adv. Colloid Interface Sci. **157**, 61–74 (2010). https://doi.org/10.1016/j.cis.2010.03.003
28. B. Rotenberg, A.J. Patel, D. Chandler, Molecular explanation for why talc surfaces can be both hydrophilic and hydrophobic. J. Am. Chem. Soc. **133**, 20521–20527 (2011). https://doi.org/10.1021/ja208687a
29. A. Phan, T.A. Ho, D. Cole et al., Molecular structure and dynamics in thin water films at metal oxide surfaces: magnesium, aluminum, and silicon oxide surfaces. J. Phys. Chem. C **116**, 15962–15973 (2012). https://doi.org/10.1021/jp300679v
30. L. Zhao, C. Wang, J. Liu et al., Reversible state transition in nanoconfined aqueous solutions. Phys. Rev. Lett. **112**, 078301 (2014). https://doi.org/10.1103/PhysRevLett.112.078301
31. L. Zhao, C.L. Wang, H.P. Fang et al., The gibbs-free-energy landscape for the solute association in nanoconfined aqueous solutions. Nucl. Sci. Tech. **26**, 030504 (2015). https://doi.org/10.13538/j.1001-8042/nst.26.030504
32. C. Wang, L. Zhao, D. Zhang et al., Upright or flat orientations of the ethanol molecules on a surface with charge dipoles and the implication for wetting behavior. J. Phys. Chem. C **118**, 1873–1878 (2014). https://doi.org/10.1021/jp4062016
33. X. Nie, J. Chen, N. Sheng et al., Effect of water molecules on nanoscale wetting behaviour of molecular ethanol on hydroxylated SiO_2 substrate. Mol. Simul. **43**, 1377–1384 (2017). https://doi.org/10.1080/08927022.2017.1353692
34. R.T. Cygan, J.-J. Liang, A.G. Kalinichev, Molecular models of hydroxide, oxyhydroxide, and clay phases and the development of a general force field. J. Phys. Chem. B **108**, 1255–1266 (2004). https://doi.org/10.1021/jp0363287
35. X. Ren, B. Zhou, C. Wang, Water-induced ethanol dewetting transition. J. Chem. Phys. **137**, 024703 (2012). https://doi.org/10.1063/1.4733719
36. X. Ren, C. Wang, B. Zhou et al., Ethanol promotes dewetting transition at low concentrations. Soft Matter **9**, 4655–4660 (2013). https://doi.org/10.1039/C3SM00049D
37. W.L. Jorgensen, D.S.M. And, J. Tiradorives, Development and testing of the opls all-atom force field on conformational energetics and properties of organic liquids. J. Am. Chem. Soc. **118**, 11225–11236 (1996). https://doi.org/10.1021/ja9621760
38. D. Van Der Spoel, E. Lindahl, B. Hess et al., Gromacs: fast, flexible, and free. J. Comput. Chem. **26**, 1701–1718 (2005). https://doi.org/10.1002/jcc.20291
39. C.-J. Shih, Q.H. Wang, S. Lin et al., Breakdown in the wetting transparency of graphene. Phys. Rev. Lett. **109**, 176101 (2012). https://doi.org/10.1103/PhysRevLett.109.176101
40. G. Vazquez, E. Alvarez, J.M. Navaza, Surface tension of alcohol water + water from 20 to 50. Degree. C. J. Chem. Eng. Data **40**, 611–614 (1995). https://doi.org/10.1021/je00019a016